






Distinct leaf water potential regulation of tree species and vegetation types across the Cerrado–Amazonia transition

Halina Soares Jancoski¹ | Beatriz Schwantes Marimon¹  | Marina C. Scalon²  |
 Fernanda de V. Barros^{3,4}  | Ben Hur Marimon-Junior¹ | Eder Carvalho¹ |
 Rafael S. Oliveira^{4,5}  | Imma Oliveras Menor^{1,6,7} 

¹Programa de Pós-graduação em Ecologia e Conservação, Universidade do Estado de Mato Grosso, Campus de Nova Xavantina, Nova Xavantina, Brazil

²Programa de Pós-graduação em Ecologia e Conservação, Universidade Federal do Paraná, Curitiba, Brazil

³Department of Geography, College of Life and Environmental Sciences, University of Exeter, Exeter, UK

⁴Programa de Pós Graduação em Ecologia, Institute of Biology, Universidade Estadual de Campinas, Campinas, Brazil

⁵Department of Plant Institute of Biology, University of Campinas, Campinas, Brazil

⁶School of Geography and the Environment, Environmental Change Institute, University of Oxford, Oxford, UK

⁷AMAP (Botanique et Modélisation de l'Architecture des Plantes et des Végétations), CIRAD, CNRS, INRA, IRD, Université de Montpellier, Montpellier, France

Correspondence

Imma Oliveras Menor and Halina S. Jancoski, Programa de Pós-graduação em Ecologia e Conservação, Universidade do Estado de Mato Grosso, Campus de Nova Xavantina, Nova Xavantina, Mato Grosso, 78690-000, Brazil.
 Emails: imma.oliveras@ouce.ox.ac.uk (I. O.); floramarela1@yahoo.com.br (H. J.)

Funding information

CAPES Science Without Borders, Grant/Award Number: 223211/2014; PELD/CNPq, Grant/Award Number: 403725/2012-7 and 441244/2016-5

Associate Editor: Jennifer Powers

Handling Editor: Norbert Kunert

Abstract

The Cerrado–Amazonia transition harbors forest and savanna formations under the influence of pronounced climate seasonality; however, the water use strategies of this key region is not yet well understood. This study aimed at deciphering in intra- and interspecific variability in leaf water potential regulation among species across three distinct vegetation types (typical cerrado, cerradão, and semideciduous seasonal forest) of the Cerrado–Amazonia transition region. We expected a variation across iso/anisohydric strategies driven by plant–environment interactions and by species attributes (phenology and wood density). We selected 21 dominant species (seven per vegetation type), recorded their phenological strategy and wood density, and measured leaf water potential (Ψ_l) during the dry and rainy seasons to analyze variations associated with minimum Ψ_l , predawn Ψ_l ($\Delta\Psi_{pd}$), and midday Ψ_l ($\Delta\Psi_{md}$) under the effect of variable vapor pressure deficit (VPD). The variation in Ψ_l across species was higher in the dry season than in the rainy season for all vegetation types. Most species from typical cerrado and cerradão showed similar behavior patterns, with higher Ψ_l regulation under high VPD and lower $\Delta\Psi_{pd}$. In contrast, most forest species showed lower regulation under high VPD, and higher $\Delta\Psi_{pd}$. Total or partial deciduousness together with strong stomatal regulation seems to be common water regulation strategies in the dry season for cerrado species but not for forest species. Our results suggest that, if drought events become more intense and frequent as predicted, seasonal forest species may be more vulnerable due to their lower Ψ_l regulation.

Abstract in Portuguese is available with online material.

KEYWORDS

drought, forest, hydraulic strategies, Neotropical, phenology, savanna, vapor pressure deficit

This is an open access article under the terms of the Creative Commons Attribution-NonCommercial-NoDerivs License, which permits use and distribution in any medium, provided the original work is properly cited, the use is non-commercial and no modifications or adaptations are made.

© 2022 The Authors. *Biotropica* published by Wiley Periodicals LLC on behalf of Association for Tropical Biology and Conservation.

1 | INTRODUCTION

Species distributions occur along gradients of water availability, with complex interactions between community composition and physiological responses of individual species to a given environmental change (Aguirre Gutiérrez et al., 2019). Thus, a marked seasonality in water will favor plants with traits and ecological strategies that enhance survival under such circumstances (Franco et al., 2005). Hence, plants occurring in highly seasonal habitats will display specialized mechanisms for water acquisition, maintenance, and use, to guarantee a favorable water balance during periods of low water availability (Oliveira et al., 2014).

The most common water transport pathway in plants occurs from the soil to the air (i.e., the continuous soil–plant–atmosphere) (Tyree, 2003), where water flows from less to more negative water potentials, establishing a difference of potentials through a water potential gradient (Larcher, 1995; Oliveira et al., 2014). The leaf water potential (Ψ_l) reflects the tension in which the xylem transports water, and it is a useful variable to infer the water status of the plant. Leaf water potentials are influenced by two main abiotic factors, by the atmospheric evaporative demand and the water availability in the soil (Oliveira et al., 2005; Palhares et al., 2010). High vapor pressure deficits (VPD) during the dry season expose plants to stressful conditions (Prado et al., 2004) and require effective stomatal regulation processes to avoid excessive water loss and regulate plant water transport (Larcher, 1995; Martínez-Vilalta et al., 2014). Based on the mechanism of transpiration regulation over time, species can be classified along a continuum of variation between two extreme strategies: isohydric species, which adjust their stomatal opening to avoid significant drops in Ψ_l , with increasing water stress (Martínez-Vilalta & Garcia-Forner, 2017). At the other extreme, anisohydric species do not adjust their stomata opening with increasing water stress, and thus, their Ψ_l declines with increasing water stress (Jones, 1998; Ratzmann et al., 2019; Tardieu & Simonneau, 1998).

The Cerrado–Amazonia transition has a strongly seasonal climate and a wide range of vegetation types, ranging from open savannas with highly diurnal temperatures and solar radiation, to closed-canopy formations with high moisture and the presence of Amazon forest species (Marimon et al., 2006, 2014). The dry season in the Cerrado, which usually extends from May to October, is characterized by low air relative humidity and high evaporative demand. At the same time in the dry season, soil dries from the surface downwards, and soil water potentials in the near-surface layers can reach values below -3.0 MPa (Franco, 2002). Although some authors suggest that many woody species from cerrado have deep roots and can access deep soil moisture throughout the year (Bucci et al., 2008; Oliveira et al., 2005), the simple access to underground water reserves does not ensure they extract enough water to compensate for the high evaporative demand during prolonged droughts (Franco et al., 2007). On the contrary, evergreen species and species in forest and transitional formations tend to have lower photosynthetic capacity (Gvozdevaite et al., 2018), stomata with high sensitivity to the increase in the atmospheric evaporative demand (Cunningham,

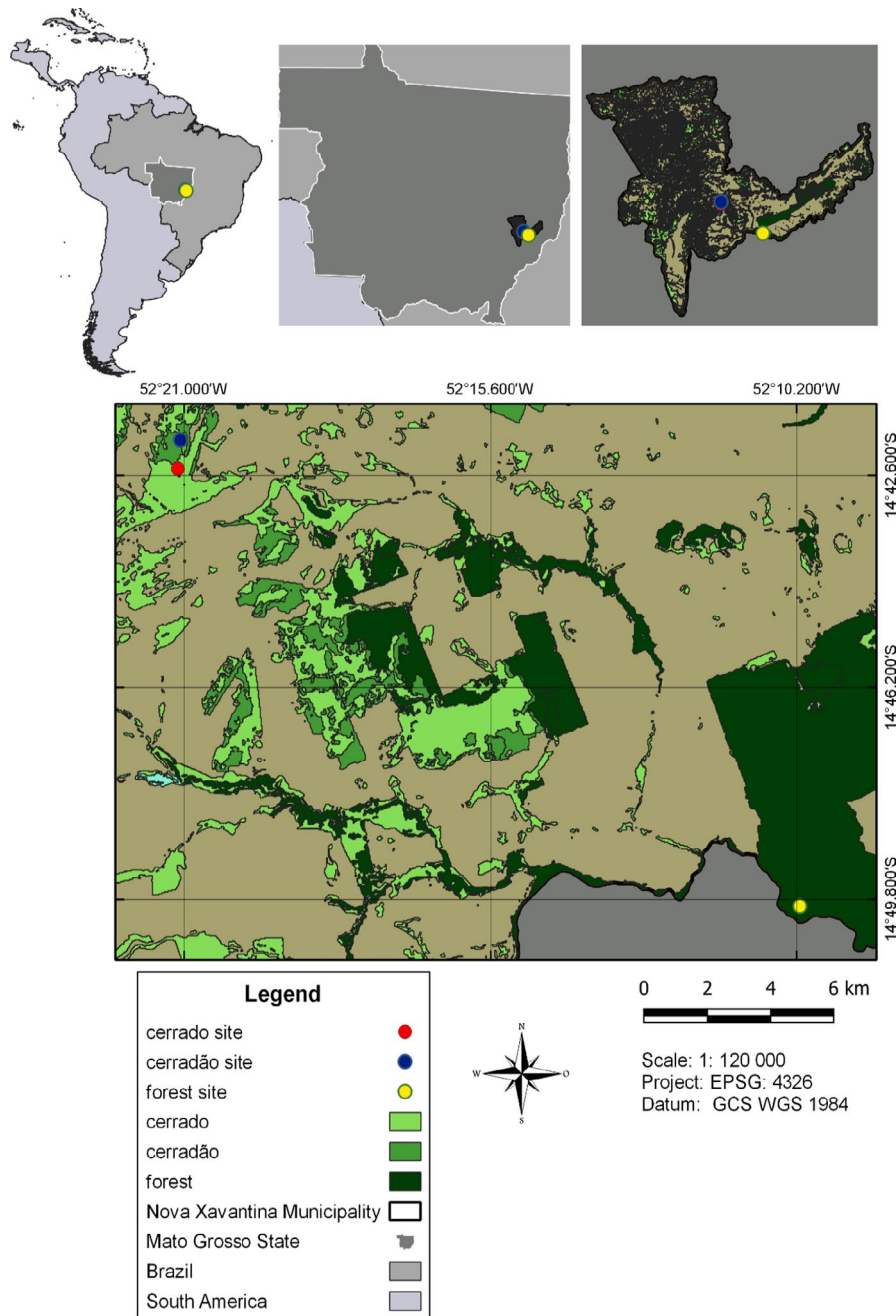
2004), and a broad range of soil water extraction patterns, from shallow-rooted to deep-rooted (Juárez et al., 2007; Oliveira et al., 2005). Hence, savanna and forest formations of the Cerrado–Amazonia transition provide a good opportunity to investigate how species from different vegetation types respond to limiting access to water. These species are under the influence of pronounced climate seasonality, high temperatures, and marked variations in humidity, which can trigger a water deficit gradient during the year (Marimon et al., 2020; Peixoto et al., 2018; Reis et al., 2018). In this highly seasonal region, Ψ_l regulation may be a distinct trait reflecting ecological strategies across species in different vegetation types. Based on the premise that physiological activity of the root system and leaf stomatal control depends on the balance between the atmospheric evaporative demand and the water availability in the soil (Oliveira et al., 2005, 2014; Palhares et al., 2010), we aim at deciphering the intra- and interspecific variability in Ψ_l regulation among species and vegetation types. We expect that the variation in iso/anisohydric strategy will respond to plant–environment interactions (Hochberg et al., 2018); that is, we expect that differences among vegetation types will be strongly driven by differences in VPD across vegetation types. We expect that most dominant species in closed-canopy vegetation types (i.e., forest and cerrado) will have low regulation of leaf water potentials (i.e., anisohydric behavior), while most dominant species in open environments (typical cerrado) will have stronger leaf water regulation mechanisms, that is, isohydric behavior. However, we do expect species-specific responses to leaf water regulations driven by phenology and wood density, with deciduous and brevideciduous species being less conservative in water use and thus showing a lower leaf water potential regulation (i.e., anisohydric strategy) to compensate for their short leaf longevity. Similarly, we would expect tendency of species with low wood density to have also more acquisitive, low leaf regulation strategy, but we expected this effect to be lower than of leaf phenology.

2 | MATERIALS AND METHODS

2.1 | Study area

The studied areas are located in southern Amazonia, in the transition between Cerrado and Amazonia biomes, state of Mato Grosso, Nova Xavantina municipality (Figure 1). The climate is Aw, according to Köppen's classification (Kottek et al., 2006), with well-defined wet (October–March) and dry (April–September) seasons. Between 2000 and 2017, the average annual rainfall was 1364 mm, with a minimum of 957.1 mm (2007) and the maximum of 1858 mm (2006) (INMET, 2018). The average annual temperature recorded in this period was 26.3°C, with the lowest average annual temperature recorded in 2003 and 2007 (18°C) and the highest in 2007 (34.5°C). Between 1997 and 2019, this region also presented a general trend of markedly increasing temperature and declining precipitation, with more negative maximum cumulative water deficit values (Marimon et al., 2020).

FIGURE 1 Location of study areas (typical cerrado; Cerradão; forest: semideciduous seasonal forest) in reference to Brazil, Mato Grosso State, and Nova Xavantina Municipality. Data base: MMA (Ministry of the Environment; site: mapas.mma.gov.br)



There is a marked difference in vegetation types in the study area, with distinct vegetation types and species composition comprising typical savanna and forest formations (Marimon et al., 2014). We assessed three contrasting vegetation types: savanna (typical cerrado—STC, Figure S1), transitional tall savanna woodland community (cerradão—SCF, Figure S2), and forest (semideciduous seasonal forest—SSF; Figure S3). Typical cerrado and SCF occur in the Bacaba Municipal Park (14°41' S; 52°20' W), while SSF is located at Vera Cruz Farm (14°49'27.1" S; 52°10'2.9" W), 25 km away from the other two (Figure 1). We carried out the study in 1-ha permanent plots that belong to the long-term monitoring projects PELD (Transição Cerrado—Amazônia: bases ecológicas e socioambientais para a conservação) and RAINFOR (<http://www.forestplots.net>).

The STC is a cerrado stricto sensu subtype with predominantly arboreal–shrubby vegetation, 20 to 50% of tree cover, and tree heights between 3 and 6 m (Ribeiro & Walter, 1998). The SCF is characterized by mostly continuous canopy with xeromorphic aspects, being considered an ecotonal community (Ratter, 1971), with species (e.g., *Hirtella glandulosa* and *Emmotum nitens*) that characterize the transition between forests and savannas on the southern Amazonian border (Marimon et al., 2006). The SSF is characterized by tall and closed-canopy vegetation and well-defined vertical strata (Askew et al., 1970; Marimon et al., 2006). The STC and SCF have Red-Yellow Latosols, dystrophic, acidic, and allic soils (Marimon-Junior & Haridasan, 2005), and the SSF has Plinthosols (Marimon et al., 2014). The characteristics of the soils of the STC and SCF vegetations are very similar with the biggest

difference being the percentage of gravel in the top 10 cm (28% in STF and 18% in STC). The properties of the STC are as follows: Al (0.9 cmol (+) kg⁻¹), Ca (0.26 cmol (+) kg⁻¹), Mg (0.5 cmol (+) kg⁻¹), P (0.33 mg kg⁻¹), and Mg/Ca ratio (0.4). The properties of SFC are as follows: Al (1.2 cmol (+) kg⁻¹), Ca (0.3 cmol (+) kg⁻¹), Mg (0.6 cmol (+) kg⁻¹), P (0.26 mg kg⁻¹), and Mg/Ca ratio (0.3) (Marimon-Junior & Haridasan, 2005). The soil in the SSF has more than 28% gravel in the top 10 cm. This value progressively increases until it forms an almost continuous semiconcretionary rock of hydromorphic laterite at approximately 90-cm depth. It has Al (0.74 cmol (+) kg⁻¹), Ca (0.66 cmol (+) kg⁻¹), Mg (1.09 cmol(+) kg⁻¹), K (0.21 cmol(+) kg⁻¹), P (3.18 mg kg⁻¹), and Mg/Ca ratio (1.8) (Marimon-Junior et al., 2019). Climate conditions were fairly similar in the different vegetation types, with mean temperatures of 31°C in the rainy season and 34.4°C in the dry season, and relative humidity oscillating between 31.5% in the dry season and 68% in the wet season (see Table 3 for a more detailed characterization of vapor pressure deficit among vegetation types and time of the year).

2.2 | Species selection

To assess leaf water regulation patterns, we selected the seven most representative species in each area, which showed the largest basal area contribution in the community, comprising a total of 21 species. In the STC, we choose adult trees with at least 5 cm in diameter at breast height (dbh), and in SCF and SSF, we selected trees with ≥10 cm of dbh. Data for tree height and dbh were extracted from census performed in 2015. Species-specific wood density data were extracted from RAINFOR data base for the studied plots (RAINFOR contains plot-specific field-collected data). Phenology was determined by B.S. Marimon (data not published).

The different vegetation types studied had a distinct composition in dominant species (Table 1). The seven studied species at STC represented 34.7% of the total basal area, with the most dominant species *Qualea parviflora* representing almost 10% of the total plot's basal area and the least dominant species representing 3.4% (*Qualea grandiflora*). The STC was the only vegetation type with fully deciduous species (three deciduous species, two brevideciduous, and two evergreen). Most species were relatively small trees (height average 5.9 ± 1.5 m), with the tallest species *Roupala montana* having average tree size of 11.2 ± 4.1 m and the smallest *Davilla elliptica* having average tree size of 3.0 ± 1.0 m (Table 1). In the SCF, the dominant studied species represented 64.1% of the total basal area, with the most dominant species *Hirtella glandulosa* representing 20.5% of the total plot's basal area and the least dominant species representing 4.3% (*Eriotheca gracilipes*). The SCF had six evergreen and one brevideciduous species, and average tree size was 9.0 ± 2.9 m; less variation was found in average tree size by species than in the STC (Table 1). The SSF plot's studied species represented 49.3% of the total plot's basal area, with the most dominant species *Ephedranthus parviflorus* representing 10% of the total plot's basal area, and the least dominant *Brosimum rubescens* representing 3.3% of the total plot's basal

area. There were five evergreen and two brevideciduous species, and the tree height averaged 11.0 ± 3.0 m (Table 1).

2.3 | Measurements of leaf water potential (Ψ_l)

In August 2016 (peak of the dry season) and January, February, and March 2017 (rainy season—measurements for each individual were conducted only once for the period), we measured the Ψ_l in two leaves of five individuals from each species, using a pressure chamber (PMS Instruments Co.; model: 1505D-EXP; Scholander et al., 1965). Measurements were taken at four different times during the day: predawn (0400–0600 GMT-4), early morning (0700–0900 GMT-4), late morning (1000–1130 GMT-4), and midday (1200–1400 hours GMT-4) in all vegetation types. We selected healthy and mature leaves, exposed to the sun at about 2.5–3.5 m height in the STC and SCF sites, and about 3–4 m in the SSF site. We also measured the temperature and relative humidity with a portable weather station (Kestrel 3500) in the vicinity of trees and where the leaves were collected. With these data, we calculated the vapor pressure deficit (VPD) in each vegetation type (Abteu & Melesse, 2013).

2.4 | Data analysis

We analyzed leaf water potential regulation at two levels: species and vegetation types. We adopted the terminology of maximum water potential value (Ψ_{max}) for the least negative potentials and the minimum water potential value (Ψ_{min}) for the most negative potentials of the day. We performed all analyses in the R 4.0.1 environment (R Core Team, 2020) and considered p -value < .05.

We determined the relationship between predawn (Ψ_{pd}) and midday (Ψ_{md}) leaf water potential, for all species and vegetation types, to access Ψ_l regulation. We used the linear model proposed by Martínez-Vilalta et al. (2014), $\Psi_{md} = \Lambda + \sigma * \Psi_s$, where Ψ_s is the soil water potential, which we considered to be similar to Ψ_{pd} (Brum et al., 2017; Larcher, 1995; Tardieu & Simonneau, 1998); σ represents the slope angle and is a proxy of the transpiration sensitivity to changes in water availability. For each species, we analyzed this relationship using the model $\Psi_{md} \sim \Psi_{pd} + (\Psi_{pd} | \text{individuals})$. Individuals of each species were included as random and fixed effects in the model to estimate the values of slopes (σ) and intercepts (Λ) of the specific relationships between Ψ_{md} and Ψ_{pd} for each species. We measured each set of individuals of a given species under the same environmental conditions. Next, we classified species as strict isohydric if the σ value and its confidence interval (CI; defined as $\sigma \pm 1$) included zero ($\sigma = 0$), strict anisohydric if the CI of σ included 1 ($\sigma = 1$), partially isohydric if CI did not include 0 and 1 ($0 < \sigma < 1$), and extreme anisohydric if CI did not include 1 ($\sigma > 1$) (Martínez-Vilalta et al., 2014). For each species and communities, we also inferred the control of water potential through $\Delta\Psi_{md}$, which is the difference between the minimum Ψ_l at midday in the rainy season and the minimum Ψ_l in the dry season (Martínez-Vilalta & Garcia-Forner, 2017). We also used

TABLE 1 Mean values of hydraulic traits for each species sampled in typical cerrado (STC), cerrado (SCF), and semideciduous seasonal forest (SSF)

Species (family)	LP	RD	Ψ_{min}	Ψ_{pd}	Ψ_{md}	$\Delta\Psi_{pd}$	$\Delta\Psi_{md}$	WD	H	BA	Λ	σ	r^2	adj. r^2
Typical cerrado (STC)														
<i>Davilla elliptica</i> A. St.-Hil. (Dilleniaceae)	BD	4.6	-2.0 ± 0.6	-0.6 ± 0.3	-1.9 ± 0.6	-0.8 ± 0.3	-0.5 ± 1.9	0.56	3.0 ± 1.0	8.4 ± 6.4	-1.0	1.2	0.9	0.9
<i>Eriotheca gracilipes</i> (K. Schum.) A. Robyns (Malvaceae)	EG	3.5	-1.1 ± 0.3	-0.5 ± 0.2	-1.0 ± 0.3	-0.6 ± 0.7	-1.4 ± 0.3	0.36	7.0 ± 1.7	14.5 ± 6.4	-0.9	0.2	0.0	-0.0
<i>Euplassa inaequalis</i> (Pohl) Engl. (Proteaceae)	BD	4.2	-2.0 ± 0.4	-0.5 ± 0.2	-1.8 ± 0.5	-0.4 ± 0.1	-1.0 ± 1.1	0.62	6.3 ± 2.2	18.7 ± 10.9	-1.0	1.3	0.2	0.2
<i>Guapira graciliflora</i> (Mart. ex Shum.) Lundell (Nyctagin.)	DE	3.7	-2.3 ± 0.8	-1.1 ± 1.0	-2.3 ± 0.7	-1.9 ± 1.6	-0.3 ± 0.1	0.52	4.4 ± 1.2	8.7 ± 3.3	-1.6	0.5	0.5	0.4
<i>Qualea parviflora</i> Mart. (Vochysiaceae)	DE	9.6	-1.7 ± 0.6	-0.6 ± 0.3	-1.6 ± 0.6	-0.5 ± 0.2	-1.4 ± 0.5	0.64	4.5 ± 1.4	16.0 ± 3	-1.2	0.7	0.1	0.0
<i>Qualea grandiflora</i> Mart. (Vochysiaceae)	DE	3.4	-2.8 ± 0.9	-1.0 ± 0.8	-2.7 ± 0.9	-1.5 ± 0.6	-1.2 ± 0.5	0.70	4.8 ± 1.2	10.6 ± 4.1	-1.8	0.8	0.4	0.4
<i>Roupala montana</i> (Klotzsch) K.S. Edwards (Proteaceae)	EG	5.7	-2.4 ± 0.4	-0.5 ± 0.2	-2.3 ± 2.4	-0.4 ± 0.1	-0.8 ± 0.5	0.78	11.2 ± 1.7	11.2 ± 4.1	-1.8	0.9	0.2	0.1
Cerrado (SCF)														
<i>Eriotheca gracilipes</i> (K. Schum.) A. Robyns (Malvaceae)	EG	4.3	-0.9 ± 0.4	-0.4 ± 0.2	-0.9 ± 0.4	-1.5 ± 2.4	-0.3 ± 0.9	0.36	10.6 ± 2.9	16.0 ± 9.3	-0.9	0.0	0.0	0.0
<i>Emmotum nitens</i> (Benth.) Miers. (Metteniusaceae)	EG	7.5	-1.8 ± 0.5	-0.9 ± 0.6	-1.6 ± 0.5	-0.9 ± 0.5	-1.4 ± 0.6	0.93	8.9 ± 4.4	15.1 ± 8.0	-1.0	0.6	0.4	0.3
<i>Hirtella glandulosa</i> Spreng. (Chrysobalanaceae)	EG	20.5	-1.6 ± 0.3	-0.5 ± 0.2	-1.5 ± 0.3	-0.4 ± 0.4	-0.3 ± 0.4	0.68	8.5 ± 2.2	12.5 ± 7.1	-1.1	0.8	0.4	0.3
<i>Myrcia splendens</i> (Sw.) DC (Myrtaceae)	EG	4.4	-2.5 ± 0.6	-1.0 ± 0.5	-2.3 ± 0.7	-0.9 ± 0.7	-0.8 ± 0.5	0.80	7.1 ± 1.8	7.5 ± 4.3	-1.5	0.8	0.4	0.3
<i>Tachigali vulgaris</i> L.G. Silva & H.C. Lima (Fabaceae)	EG	17.4	-2.4 ± 0.5	-0.9 ± 0.3	-2.4 ± 0.5	-0.6 ± 0.3	-1.2 ± 0.5	0.61	10.4 ± 3.3	9.5 ± 7.0	-1.3	1.4	0.7	0.7
<i>Tapirira guianensis</i> Aubl. (Anacardiaceae)	BD	5.2	-1.4 ± 0.6	-0.9 ± 0.6	-1.3 ± 0.5	-1.1 ± 0.8	-1.6 ± 0.9	0.45	9.2 ± 2.6	9.2 ± 5.2	-0.9	0.4	0.2	0.1
<i>Xylopia aromatica</i> (Lam.) Mart. (Annonaceae)	EG	4.8	-2.0 ± 0.5	-0.6 ± 0.3	-2.0 ± 0.5	-0.6 ± 0.5	-1.0 ± 0.6	0.56	8.0 ± 2.8	8.5 ± 5.9	-1.6	0.6	0.1	0.0
Semideciduous-seasonal forests (SSF)														
<i>Amaioua guianensis</i> Aubl. (Rubiaceae)	EG	7.7	-2.3 ± 1.5	-1.6 ± 1.5	-2.5 ± 1.4	-2.0 ± 1.4	-2.1 ± 1.2	0.67	9.7 ± 2.7	13.0 ± 6.2	-1.1	0.8	0.9	0.9
<i>Brosimum rubescens</i> Taub. (Moraceae)	EG	3.3	-1.4 ± 0.8	-0.8 ± 0.4	-1.3 ± 0.8	-1.9 ± 1.3	-3.3 ± 0.6	0.80	11.6 ± 4.0	16.4 ± 10.3	0.1	1.8	0.7	0.6
<i>Chaetocarpus echinocarpus</i> (Baill.) Ducke (Peraceae)	EG	9.4	-2.4 ± 1.3	-1.4 ± 1.3	-2.2 ± 1.2	-1.8 ± 1.5	-2.3 ± 1.1	0.79	12.9 ± 3.3	19.5 ± 7.0	-1.0	0.8	0.9	0.9
<i>Cheiloclinium cognatum</i> (Miers.) A.C. Sm. (Celastraceae)	BD	3.9	-2.1 ± 1.5	-0.7 ± 0.4	-2.1 ± 1.4	-0.8 ± 0.5	-1.5 ± 0.7	0.63	7.4 ± 2.10	12.8 ± 3.3	-0.0	2.9	0.7	0.7
<i>Ephedranthus parviflorus</i> S. Moore (Annonaceae)	EG	10	-2.4 ± 1.4	-1.1 ± 0.8	-2.2 ± 1.2	-1.6 ± 0.4	-2.5 ± 0.4	0.73	12.0 ± 3.4	17.4 ± 6.2	-0.9	1.3	0.6	0.6
<i>Mabea fistulifera</i> Mart. (Euphorbiaceae)	BD	6.4	-1.7 ± 1.1	-0.7 ± 0.6	1.0	-1.7 ± 1.2	-2.5 ± 1.0	0.61	12.3 ± 2.2	12.5 ± 5.6	-0.8	2.0	0.2	0.1
<i>Protium altissimum</i> (Aubl.) Marchand (Bursaceae)	EG	8.6	-1.7 ± 1.0	-0.8 ± 0.6	-1.5 ± 1.0	-1.0 ± 0.4	-2.2 ± 1.3	0.70	11.2 ± 3.0	17.3 ± 10.7	-0.6	1.2	0.4	0.3

Note: Leaf phenology (LP) is classified as brevideciduous (BD), deciduous (DE) or evergreen (EG), wood density (WD, g cm⁻³), height (H, m), basal area (BA, m²), and species relative dominance (RD) in each community. Hydraulic traits: minimum Ψ_i (Ψ_{min}); Ψ_i at predawn (Ψ_{pd}); Ψ_i at midday (Ψ_{md}); variation of predawn Ψ_i ($\Delta\Psi_{pd}$); and variation of Ψ_i at midday ($\Delta\Psi_{md}$); slope angle (σ) and intercept (Λ) between the ratio of the leaf water potential (Ψ_i , MPa) at predawn (Ψ_{pd}) and midday (Ψ_{md}), marginal (r^2) and conditional coefficient of correlation of each model (adj. r^2). Species-specific individual slopes are shown in Figure S6.

the variation in Ψ_{pd} ($\Delta\Psi_{pd}$), calculated by the difference between Ψ_{pd} in the rainy season and dry season, to estimate the root depth of species in relation to the water availability in the soil (Scholz et al., 2012). For this latter step, we used the modular values of the deltas.

To perform analyses at the vegetation-type level, we calculated the basal area-weighted average for each attribute (Ψ_{min} , $\Delta\Psi_{pd}$, $\Delta\Psi_{md}$, and σ). We also calculated the relative dominance in the basal area of the species, which corresponds to the species-specific total basal area dividing by the total plot basal area (i.e., the sum of the basal areas of all species in the plot) (Shepherd, 2010). We used the *weights*, *quantreg*, and *Hmisc* packages (R Core Team, 2020).

We explored whether Ψ_i varied between species and among the four different periods of the day assessed in each season (dry and rainy). Then, we tested whether Ψ_i and other hydraulic traits (Ψ_{min} , $\Delta\Psi_{pd}$, and $\Delta\Psi_{md}$) varied among the vegetation types and the different seasons (dry and rainy). For the analyses, we used Kruskal–Wallis non-parametric test, followed by the Dunn test as a post hoc analysis, since data did not follow normality assumptions for parametric tests. We used *plyr*, *dunn.test*, and *FSA* packages (Dunn, 1964; Wickham, 2011).

We further explored whether any potential differences in Ψ_i across species and vegetation types were driven by VPD by performing linear regression analysis for each species, vegetation type, and season. We then compared linear regression curves for the bivariate relationship of Ψ_i and VPD between different vegetation types (standardized major axis–SMA), using the *smatr* package (Warton et al., 2012), for log-10 transformed variables.

To examine the amount of hydraulic trait variation explained across different nested scales, we partitioned variance within and among vegetation types, phenological groups, and species. The decomposition of variance followed Messier et al. (2010), using the package *cati* (Taudiere & Violle, 2015).

We used generalized linear mixed models to understand the influence of vegetation type, phenological groups, and wood density (fixed effects) in the variation in Ψ_{pd} and Ψ_{md} , as well as the slope angle (σ), with species as random effect. We built different models for each response variable using package *lme4* and compared group means using packages *car* and *emmeans*.

3 | RESULTS

3.1 | Effect of seasonality on Ψ_i

We found a broad variation in Ψ_i among species and vegetation types (Table 1). The Ψ_{min} varied from -2.8 ± 0.9 MPa (*Q. grandiflora*) to -0.9 ± 0.4 MPa (*E. gracilipes*). Most species had an average Ψ_{pd} between 0 and -1 (Table 1), although three out of the seven species studied in SSF had average Ψ_{pd} below -1 (*Amaioua guianensis*, *Chaetocarpus echinocarpus*, and *E. parviflorus*). In case of *A. guianensis*, this was because this species recorded the most negative Ψ_{pd} during the dry period (-3.5 ± 0.9 MPa) among all species (Figure S4). Most species showed Ψ_{pd} below -1 MPa during the dry season (Figure

S4), except for *E. gracilipes* (-0.54 ± 0.23 MPa), *Euplassa inaequalis* (-0.73 ± 0.08 MPa), and *R. montana* (-0.81 ± 0.15 MPa), all species occurring at the STC vegetation type. There was much more variation in Ψ_{md} than in Ψ_{pd} among species in both the rainy and dry seasons. In the rainy season, *Myrcia splendens* exhibited the lowest Ψ_{md} (-2.0 ± 0.6 MPa), and in the dry season, *A. guianensis* consistently exhibited the most negative values (-4.0 ± 0.3 MPa), although *C. echinocarpus* and *Q. grandiflora* also occasionally reached negative values up to -4 MPa (Figure S4). Overall, species from the SSF vegetation type had largest $\Delta\Psi_{md}$ (except for *C. echinocarpus*; Table 1).

Regarding communities, in the rainy season, Ψ_i values in the forest vegetation type remained higher than those of other vegetation types (Figure 2a; SSF and SCT–dry season: $Z = 4.48$; $p < .001$ and rainy season: $Z = -3.94$; $p < .001$; and SSF and STF–dry season: $Z = 1.97$; $p < .001$ and rainy season: $Z = 3.89$; $p < 1$ 0.00). In contrast, in the dry season, the forest vegetation type showed the lowest mean values of Ψ_i at all times of the day, with a continuous decrease from predawn to midday ($p < .05$ for all tests, Figures 2b and S5). Regarding the Ψ_i variability across the year, we observed a significantly higher $\Delta\Psi_{pd}$ (Dunn test, $Q_2 = 16.92$, $df = 2$, $p < .001$) and $\Delta\Psi_{md}$ in SSF compared with other vegetation types ($Q_2 = 3.72$, $df = 2$, $p < .001$, Figures 2c and S5).

3.2 | Regulation of Ψ_i

We observed that 47% of the study species are partially isohydric, and 43% are extreme anisohydric (Figure 3). *E. gracilipes* was the only strict isohydric species, which showed the same pattern in both typical STC and SCF (Figure S6). This species showed a slope coefficient $\sigma = 0$, very low correlation coefficient values (Table 1, Figure S6), and it was the only species for which σ coefficient value was not significant ($p > .1$). Therefore, we performed subsequent linear mixed models both with and without it.

When separated by vegetation types, we observed that 57% of species in STC and SCF were partially isohydric, whereas most species in SSF were extremely anisohydric (71%). We also found that all deciduous species were partially isohydric, while evergreen and brevideciduous species varied among vegetation types (Table 1). The SSF species, *Cheilochlinium cognatum*, and the STC and SCF species, *E. gracilipes*, represented the opposite extremes in Ψ_i regulation (i.e., they were the most strictly anisohydric and isohydric respectively, Figures 3 and S6, Table 1).

The $\Delta\Psi_{pd}$ and $\Delta\Psi_{md}$ differed between vegetation types (Table 2, Figure 4), with the species from SSF being the ones that showed the least regulation (Table 1), that is, the higher $\Delta\Psi_{pd}$ and $\Delta\Psi_{md}$. The difference between vegetation types was maintained whether the species *E. gracilipes* was included (Table 3, Figure 4) or not included in the analyses (Table S1, Figure S7).

Leaf phenology influenced both $\Delta\Psi_{pd}$ and σ , with deciduous species showing lower values, while brevideciduous species showed higher values and evergreen intermediate values (Figure 4, Table 3). Wood density only influenced σ , where species with denser wood

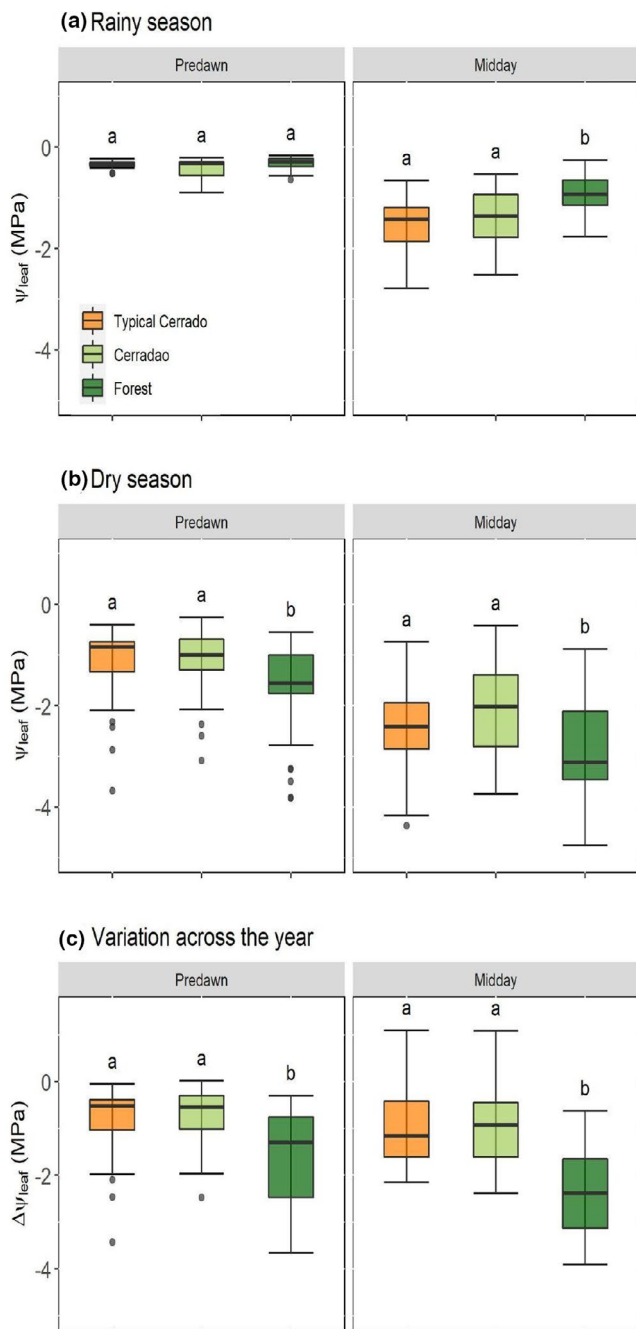


FIGURE 2 Leaf water potential (Ψ_{leaf} , MPa) at predawn (0400–0600 h GMT-4) and at midday (1200–1400 h GMT-4) in the different vegetation types (typical cerrado (STC)—orange boxes, cerradão (SCF)—light green boxes; and semideciduous seasonal forest (SSF)—dark green boxes) for the (a) rainy and (b) dry seasons. (c) Variation across the year in Ψ_i at predawn and the variation in Ψ_i at midday. Boxplots showing median and 25° and 75° percentiles. Different letters show statistical differences between vegetation ($p < .05$)

showed higher slope angles, meaning that they had a more anisohydric behavior (Figure 4, Table 3). This relationship disappeared when *E. gracilipes*—that had the lowest wood density of all species—was excluded from the analysis (Table S1, Figure S7).

Overall, vegetation type explained a significant part of the variation for σ (~38%), $\Delta\Psi_{\text{pd}}$ (~19%), and $\Delta\Psi_{\text{md}}$ (~68%), even though leaf phenology also helped explaining the variation for these hydraulic traits (ranging from 2 to 32% of the variance; Figure S8). Remarkably, 100% of the variation in Ψ_{min} and Ψ_{md} was explained by species (Figure S8).

3.3 | Effect of VPD on leaf water potential (Ψ_i)

The VPD differed among vegetation types but was higher in the dry season in all areas (Table 3 and S2), with a significant negative correlation between VPD and Ψ_i (Figure 5). The SSF showed the lowest Ψ_i values and the lowest VPD amplitude in both seasons (Figure 5 and Table 3).

In the dry season, VPD in the STC was 20% higher than that recorded in the SCF, and approximately 30% higher than that of the SSF ($\text{VPD}_{\text{STC}} > \text{VPD}_{\text{SCF}} > \text{VPD}_{\text{SSF}}$), which confirms that species are subject to a higher atmospheric water demand during this season in the savanna vegetation (Table 3). We also observed a direct relationship between the decrease in Ψ_i and the increase in VPD; the SCF showed environmental variations more similar to STC than to SSF, which showed the lowest Ψ_i in the dry season (Figure 5).

Looking at species-specific responses (Figure S9), the STC species *Guapira graciliflora*, the SCF species *Tapirira guianensis*, and the shared STC and SCF species *E. gracilipes* showed the lowest response to shifts in VPD in the dry season. The species with strongest responses to changes in VPD in the dry season were *E. parviflorus* from the SSF, *R. montana* from STC, and *Xylopia aromatica* from SCF.

4 | DISCUSSION

Our results showed different strategies for water use among species and vegetation types in the Brazilian Cerrado–Amazonia transition. We observed differences between the leaf water potential regulation of forest species in relation to typical cerrado and cerradão species, which tended to show stronger leaf water potential regulation (partial isohydric strategy) than forest species (anisohydric strategy).

Our main working hypothesis was that there would be strong plant–environment interactions and that there would be more anisohydric species in the closed-canopy vegetation types (forest and cerradão) than in open-canopy vegetation types (typical cerrado). Contrary to our expectations, we found that hydraulic traits of the cerradão species were generally more similar to typical cerrado than to the semideciduous seasonal forest. Cerradão is a transitional community floristically closer to forests than savannas (Morandi et al., 2016), and its vegetation structure (e.g., tree size, phenology) was also more similar to the forest than to the typical cerrado (Table 1). The typical cerrado in our study area is turning to a dense cerrado by increasing its biomass and incorporating species that form close canopies, due to long-term fire exclusion (Morandi et al., 2016; Ribeiro & Walter, 1998).

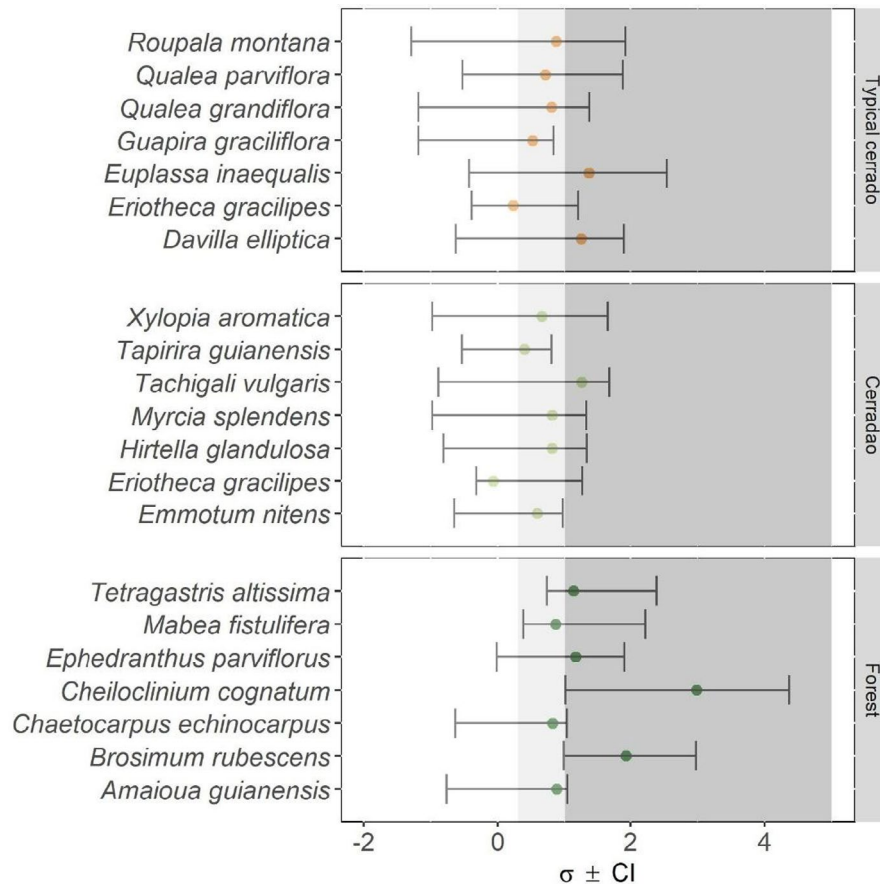


FIGURE 3 Leaf water potential regulation of 21 species divided into vegetation types: typical cerrado (STC) (orange circles), cerradão (SCF) (light green circles), and semideciduous seasonal forest (SSF) (dark green circles). The slope angle ($\sigma \pm CI$ —confidence interval) estimates the value that allows classifying the species as strict isohydric (white area), partially isohydric (light gray area), and extreme anisohydric (dark gray area). No species was identified as strict anisohydric

TABLE 2 Generalized linear model results for the variation Ψ_l at predawn ($\Delta\Psi_{pd}$); and variation of Ψ_l at midday ($\Delta\Psi_{md}$) and the slope angle (σ) of the relationship between leaf water potential at predawn (Ψ_{pd}) and midday (Ψ_{md}), with vegetation type, phenology, and wood density as fixed effects

Response variable	Source of variation	Chisq	d.f.	p-Value
$\Delta\Psi_{pd}$	Vegetation type	16.30	2	<.001
	Wood density	0.27	1	.605
	Phenology	6.93	2	.031
$\Delta\Psi_{md}$	Vegetation type	8.99	2	.011
	Wood density	1.04	1	.308
	Phenology	0.23	2	.891
σ	Vegetation type	16.90	2	<.001
	Wood density	11.78	1	<.001
	Phenology	8.15	2	.017

Note: Bold are statistically significant ($p < .05$).

On the one hand, our models corroborated a strong effect of vegetation type on the hydraulic properties studied, and the fact that both the typical cerrado and the cerradão are more similar than the cerradão and the forest suggests a strong plant–environmental filtering. Indeed, the typical cerrado and cerradão sites have similar soil properties (Marimon-Junior & Haridasan, 2005) and VPD (Table 3). On the other hand, the lower variation in the Ψ_{pd} (values

did not decrease much in the dry season) for most typical cerrado and cerradão species (compared to forest species) suggests that they may be growing with access to water in the soil (Palhares et al., 2010), and the fact that the forest site has a laterite layer at 90 cm corroborates the shallow soils of the studies forest site. Although we did not explicitly include root depth (instead used a proxy through $\Delta\Psi_{pd}$) or measured soil moisture profiles in this study, future research should explore these interactions in the Amazon–Cerrado transition, because root structure and soil moisture are key factors in plant hydraulic patterns (Oliveira et al., 2021). Deep roots are critical to maintain water balance of cerrado ecosystems (Oliveira et al., 2005), despite involving higher maintenance costs or strict control of plant water balance (Franco et al., 2005). For example, *Eriotheca gracilipes*, which showed little seasonal variation in leaf water potential, develops a main root of approximately 2.5 m in length, without many fine roots (Durigan et al., 2012). In the cerrado, brevideciduous and deciduous species have dimorphic root systems (both shallow and tap roots), while evergreen species have mostly a monomorphic root system (deep roots) (Scholz et al., 2012). In such conditions, hydraulic redistribution may also be an important operating mechanism, which has already been observed for some cerrado species included in this study such as the most dominant species in our typical cerrado site, *Qualea parviflora* and *Roupala montana* (Bucci et al., 2008; Scholz et al., 2002). However, to the best of our knowledge, there are no studies on the root systems and phenology relationships in seasonal semideciduous forest species.

FIGURE 4 Comparison between the variation of Ψ_l at predawn ($\Delta\Psi_{pd}$); and variation of Ψ_l at midday ($\Delta\Psi_{md}$) and the slope angle (σ) of the relationship between leaf water potential at predawn (Ψ_{pd}) and midday (Ψ_{md}) for the different vegetation types (typical cerrado [STC], cerradão [SCF], and semideciduous seasonal forest [SSF]), different phenological groups, and the relationship with wood density. Statistics are shown in Table 2. Boxplots showing median and 25° and 75° percentiles, and different letters show statistical differences between groups ($p < .05$). Solid lines show significant relationships ($p < .05$)

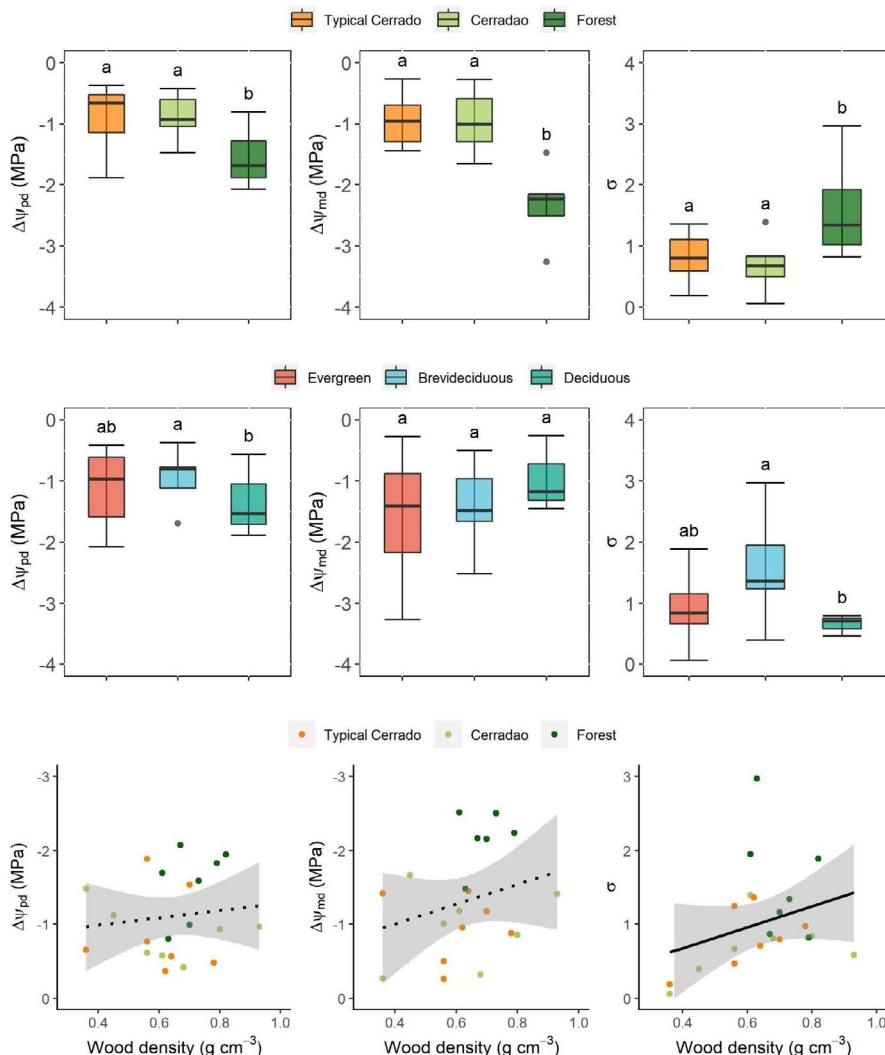


TABLE 3 Characterization of the vapor pressure deficit (KPa) of the vegetation types (STC = typical cerrado, SCF = cerradão, and SSF = semideciduous seasonal forest) in dry ($r^2 = 0.14$; $p < .001$) and rainy ($r^2 = .32$; $p < .001$) seasons

Seasons	STC	SCF	SSF
Dry			
Maximum	4.95	4.73	3.77
Minimum	0.43	0.18	0.3
Mean \pm SD	2.43 \pm 1.63	1.94 \pm 1.59	1.69 \pm 1.64
Rainy			
Maximum	2.80	3.13	1.13
Minimum	0	0	0
Mean \pm SD	0.92 \pm 1.52	0.74 \pm 1.53	0.2 \pm 1.63

On the other hand, atmospheric demand in the typical cerrado and cerradão was consistently higher than for the forest in both seasons. The stronger regulation of Ψ_l recorded for most typical cerrado and cerradão species was probably related to a more efficient regulation of stomatal opening in response to changes in VPD, shown by the fact that the most negative leaf water potentials

in typical cerrado and cerradão usually occurred at 1000 am and were maintained at 1200. This is in accordance with other studies that found strong influence of atmospheric demand variability in stomatal regulation of the community dominant species (Franco & Lüttge, 2002; Garcia et al., 2021). Indeed, many cerrado species during the dry season increase their stomatal conductance and sap flow in the early morning, followed by an acute decline in both stomatal conductance and sap flow before VPD peaks in the early afternoon (Bucci et al., 2008; Goldstein et al., 2008). Moreover, previous studies have reported that the total or partial deciduousness of most cerrado and cerradão species helps to decrease water loss by leaf transpiration in the dry season (Goldstein et al., 2008). Finally, partially or total leaf shedding in the dry season also exerts an important role in leaf water regulation as shown in this study, provided that the fewer the leaves, the lower the leaf area and thus the lower the water demand. Nonetheless, leaf shedding did not explain water regulation in the forest site because most forest species showed a lower regulation of Ψ_l with higher drop in Ψ_l and higher $\Delta\Psi_{pd}$, which might indicate that either these species have acquisitive strategies (e.g., rapid growth) or high resistance to embolism (Oliveira et al., 2021).

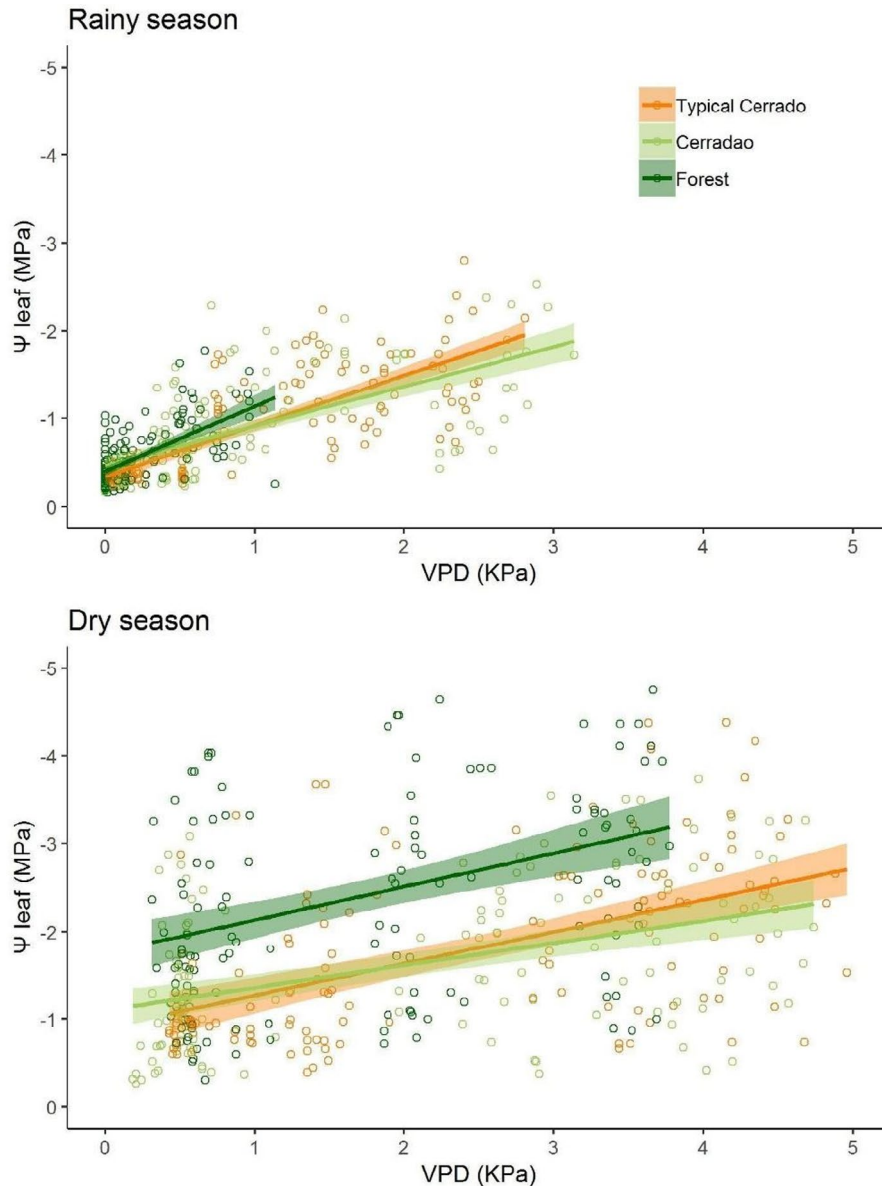


FIGURE 5 Linear regression between the leaf water potential (Ψ_l , MPa) and the vapor pressure deficit (VPD, KPa) of the typical cerrado (STC) (orange), cerradão (SCF) (light green), and semideciduous seasonal forest (SSF) (dark green), in the Cerrado–Amazonia transition, Brazil. Circles represent individuals sampled in each vegetation type. Individual slopes between regression lines differed between vegetation types in both rainy ($p < .001$) and dry seasons ($p < .001$) (standardized major axis–SMA). Individual slopes, confidence intervals, and correlation coefficients are shown in Table S2

The differences in Ψ_l among species suggest a substantial interspecific variation in hydraulic functioning regulation of the different vegetation types. Specifically, we found an effect of leaf phenology and wood density in driving the leaf water potential regulation, although this effect was lower than the effect of vegetation type (Table 3). Leaf phenology had a significant effect on $\Delta\Psi_{pd}$ and σ , with deciduous species having a more negative $\Delta\Psi_{pd}$ and σ closer to 0 than brevideciduous, but evergreen species were not different from the other strategies. Brevideciduous species are functionally evergreen because they seldom remain leafless for more than a few days (Bucci et al., 2005). The lack of difference between evergreen and the other phenological groups is probably due to the intraspecific variability within phenological groups, which we speculate that might be driven by the presence of evergreen species across the three vegetation types. Unfortunately, due to an unbalanced design (deciduous species were only present in the typical cerrado site), we could not include the interaction between vegetation type and

phenology in our models. These results are in accordance with de Souza et al. (2020), who reported intraspecific variability in water use strategies within deciduous trees in tropical seasonal dry forests of the Caatinga. Nonetheless, in the cerrado, species of the three phenological groups overlap substantially in ecophysiological characteristics (Goldstein et al., 2008). Goldstein et al. (2008) suggested that the use of functional trade-offs and syndromes was more appropriate than the use of phenological categories because the grouping of cerrado species in the latter is somewhat arbitrary, and the description of functional type typologies that represent variation along a continuum may represent better the ecological complexity resulting from the adaptations of cerrado tree species to their environment.

Other studies have reported differences between cerrado and semideciduous season forest regulation of leaf water potential (e.g., Gotsch et al., 2010), but to the best of our knowledge, this is the first study reporting the diverging leaf water regulation of cerradão

dominant species to semideciduous forest dominant species at the Amazon–Cerrado transition.

As extreme drought events become more intense and frequent in this zone of ecological tension/stress on the southern Amazonia (Marimon et al., 2014; Reis et al., 2018; Rifai et al., 2018), higher VPDs and decreases in soil moisture might impose riskier conditions for some species. Some studies have shown that, in isohydric species, xylem vessels embolize more frequently, since the Ψ_{\min} is close to P50 (i.e., Ψ_1 value in which the stem hydraulic conductivity is reduced by half), with a small safety margin (McDowell, 2011). On the contrary, these authors also noted that anisohydric species have a higher safety margin because they maintain xylem tension above the water potential values that usually cause embolism. Further research linking water use regulation strategies and xylem properties is urgently needed for the Cerrado–Amazonia transition.

5 | CONCLUSION

The hydraulic functioning of the species within the three studied vegetation types differed in response to the marked climate seasonality of the region, and to phenology. Species from the typical cerrado and cerrado showed relatively similar hydraulic strategies with partially isohydric behavior and strong leaf water regulation under high atmospheric pressure demands, while forest species had lower leaf water regulation, and our study supports the hypothesis of plant–environment interactions playing a major role in leaf water regulation and the existence of niche partitioning due to abiotic filtering (atmospheric demand).

Our study described how leaf water traits vary throughout the year for the major vegetation types that occur in the transition of the two largest South American biomes. It also advanced the knowledge of the hydraulic functioning patterns of this unique and vulnerable region, to better understand species- and community-level hydraulic responses in a future scenario of more frequent and more extreme drought events.

ACKNOWLEDGEMENTS

This project was funded by CAPES Science Without Borders Grant 223111/2014 to IO, which included a PhD CAPES scholarship to HSJ and a postdoctoral CAPES fellowship to MCS. HSJ was logistically supported by the Programa de Pós-graduação em Ecologia e Conservação of UNEMAT Campus Nova Xavantina. BHMJ and BSM were supported by a CNPq productivity scholarship and by the PELD/CNPq projects #403725/2012-7 and 441244/2016-5. RSO was supported by a CNPq productivity scholarship and by NERC-FAPESP 19/07773-1. The authors are thankful to two anonymous reviewers that helped improving the quality of the manuscript, and to the editors for their contributions to handling and proofreading it. Open Access funding enabled and organized by Projekt DEAL.

AUTHOR CONTRIBUTIONS

IO, RSO, MSC, and HSJ designed the main ideas with contribution from BSM, FB, and BHMN. IO secured funding, and BSM, BHMJ,

and RSO provided logistical support. HSJ, EC, and MCS collected data. HSJ and MCS analyzed data with support from IOM and FB. HSJ was co-supervised by IOM and BSM. HSJ, IOM and MCS wrote the manuscript with critical contributions of all authors in different versions of the manuscript and final comments and approval from all authors.

DATA AVAILABILITY STATEMENT

Data are available at Oliveras Menor and Jancoski (2021).

ORCID

Beatriz Schwantes Marimon  <https://orcid.org/0000-0003-3105-2914>

Marina C. Scalón  <https://orcid.org/0000-0003-2069-8226>

Fernanda de V. Barros  <https://orcid.org/0000-0003-3835-2020>

Rafael S. Oliveira  <https://orcid.org/0000-0002-6392-2526>

Imma Oliveras Menor  <https://orcid.org/0000-0001-5345-2236>

REFERENCES

- Abtew, W., & Melesse, A. (2013). Vapor pressure calculation methods. In W. Abtew & A. Melesse (Eds.), *Evaporation and evapotranspiration* (pp. 53–62). Springer.
- Aguirre-Gutiérrez, J., Oliveras, I., Rifai, S., Fauset, S., Adu-Bredu, S., Affum-Baffoe, K., Baker, T. R., Feldpausch, T. R., Gvozdevaite, A., Hubau, W., Kraft, N. J. B., Lewis, S. L., Moore, S., Niinemets, Ü., Peprah, T., Phillips, O. L., Ziemnińska, K., Enquist, B., & Malhi, Y. (2019). Drier tropical forests are susceptible to functional changes in response to a long-term drought. *Ecology Letters*, 22(5), 855–865. <https://doi.org/10.1111/ele.13243>
- Askew, G., Moffatt, D., Montgomery, R., & Searl, P. (1970). Interrelationships of soils and vegetation in the savanna-forest boundary zone of North-Eastern Mato Grosso. *The Geographical Journal*, 136(3), 370–376.
- Brum, M., Teodoro, G. S., Abrahão, A., & Oliveira, R. S. (2017). Coordination of rooting depth and leaf hydraulic traits defines drought-related strategies in the campos rupestres, a tropical montane biodiversity hotspot. *Plant and Soil*, 420(1–2), 467–480.
- Bucci, S. J., Goldstein, G., Meinzer, F. C., Franco, A. C., Campanello, P., & Scholz, F. G. (2005). Mechanisms contributing seasonal homeostasis of minimum leaf water potential and predawn disequilibrium between soil and plant water potential in Neotropical savanna trees. *Trees*, 19, 296–304.
- Bucci, S. J., Scholz, F. G., Goldstein, G., Hoffmann, W. A., Meinzer, F. C., Franco, A. C., Giambelluca, T., & Miralles-Wilhelm, F. (2008). Controls on stand transpiration and soil water utilization along a tree density gradient in a Neotropical savanna. *Agricultural and Forest Meteorology*, 148(6–7), 839–849. <https://doi.org/10.1016/j.agrformet.2007.11.013>
- Cunningham, S. C. (2004). Stomatal sensitivity to vapor pressure deficit of temperate and tropical evergreen rainforest trees of Australia. *Trees*, 18(4), 399–407.
- De Souza, B. C., Carvalho, E. C. D., Oliveira, R. S., De Araujo, F. S., De Lima, A. L. A., & Rodal, M. J. N. (2020). Drought response strategies of deciduous and evergreen woody species in a seasonally dry neotropical forest. *Oecologia*, 194(1–2), 221–236. <https://doi.org/10.1007/s00442-020-04760-3>
- Dunn, O. J. (1964). Multiple comparisons using rank sums. *Technometrics*, 6(3), 241–252. <https://doi.org/10.1080/00401706.1964.10490181>
- Durigan, G., Melo, A. C. G., & Brewer, J. S. (2012). The root to shoot ratio of trees from open- and closed-canopy cerrado in south-eastern Brazil. *Plant, Ecology & Diversity*, 5, 333–343. <https://doi.org/10.1080/17550874.2012.691564>

- Franco, A. C. (2002). Ecophysiology of cerrado woody plants. In P. S. Oliveira, & R. J. Marquis (Eds.), *The cerrados of Brazil: Ecology and natural history of a neotropical savanna* (pp. 178–197). Columbia University Press.
- Franco, A. C., Bustamante, M., Caldas, L. S., Goldstein, G., Meinzer, F. C., Kozovits, A. R., Rundel, P., & Coradin, V. T. R. (2005). Leaf functional traits of Neotropical savanna trees in relation to seasonal water deficit. *Trees-Structure and Function*, *19*(3), 326–335. <https://doi.org/10.1007/s00468-004-0394-z>
- Franco, A. C., & Lüttge, U. (2002). Midday depression in savanna trees: Coordinated adjustments in photochemical efficiency, photorespiration, CO₂ assimilation and water use efficiency. *Oecologia*, *131*(3), 356–365. <https://doi.org/10.1007/s00442-002-0903-y>
- Franco, A. C., Matsubara, S., & Orthen, B. (2007). Photoinhibition, carotenoid composition and the co-regulation of photochemical and non-photochemical quenching in neotropical savanna trees. *Tree Physiology*, *27*(5), 717–725. <https://doi.org/10.1093/treephys/27.5.717>
- Garcia, M. N., Ferreira, M. J., Ivanov, V., Dos Santos, V. A. H. F., Ceron, J. V., Guedes, A. V., Saleska, S. R., & Oliveira, R. S. (2021). Importance of hydraulic strategy trade-offs in structuring response of canopy trees to extreme drought in central Amazon. *Oecologia*, *197*(1), 13–24. <https://doi.org/10.1007/s00442-021-04924-9>
- Goldstein, G., Meinzer, F. C., Bucci, S. J., Scholz, F. G., Franco, A. C., & Hoffmann, W. A. (2008). Water economy of Neotropical savanna trees: Six paradigms revisited. *Tree Physiology*, *28*, 395–404. <https://doi.org/10.1093/treephys/28.3.395>
- Gotsch, S. G., Geiger, E. L., Franco, A. C., Goldstein, G., Meinzer, F. C., & Hoffmann, W. A. (2010). Allocation to leaf area and sapwood area affects water relations of co-occurring savanna and forest trees. *Oecologia*, *163*(2), 291–301. <https://doi.org/10.1007/s00442-009-1543-2>
- Gvozdevaite, A., Oliveras, I., Domingues, T. F., Peprah, T., Boakye, M., Afriyie, L., da Silva Peixoto, K., de Farias, J., Almeida de Oliveira, E., Almeida Farias, C. C., dos Santos Prestes, N. C. C., Neyret, M., Moore, S., Schwantes Marimon, B., Marimon Junior, B. H., Adu-Bredu, S., & Malhi, Y. (2018). Leaf-level photosynthetic capacity dynamics in relation to soil and foliar nutrients along forest-savanna boundaries in Ghana and Brazil. *Tree Physiology*, *38*, 1926. <https://doi.org/10.1093/treephys/tpy136>
- Hochberg, U., Rockwell, F. E., Holbrook, N. M., & Cochard, H. (2018). Iso/Anisohdry: A Plant-Environment Interaction Rather Than a Simple Hydraulic Trait. *Trends in plant science*, *23*(2), 112–120. <https://doi.org/10.1016/j.tplants.2017.11.002>
- INMET. Instituto Nacional de Meteorologia. Retrieved from <http://www.inmet.gov.br/portal> Accessed May 10, 2018.
- Jones, H. G. (1998). Stomatal control of photosynthesis and transpiration. *Journal of Experimental Botany*, *387*–398. https://doi.org/10.1093/jxb/49.Special_Issue.387
- Juárez, R. I. N., Hodnett, M. G., Fu, R., Goulden, M. L., & Von Randow, C. (2007). Control of dry season evapotranspiration over the Amazonian forest as inferred from observations at a southern Amazon forest site. *Journal of Climate*, *20*(12), 2827–2839. <https://doi.org/10.1175/JCLI4184.1>
- Kottek, M., Grieser, J., Beck, C., Rudolf, B., & Rubel, F. (2006). World map of the Köppen-Geiger climate classification updated. *Meteorologische Zeitschrift*, *15*(3), 259–263. <https://doi.org/10.1127/0941-2948/2006/0130>
- Larcher, W. (1995). *Physiological plant ecology: Ecophysiology and stress physiology of functional group* (p. 433). Springer-Verlag.
- Marimon, B. S., Lima, E. S., Duarte, T. G., Chierigatto, L. C., & Ratter, J. A. (2006). Observations on the vegetation of northeastern Mato Grosso, Brazil: An analysis of the Cerrado-Amazonian forest ecotone. *Edinburgh Journal of Botany*, *63*, 323–341.
- Marimon, B. S., Marimon-Junior, B. H., Feldpausch, T. R., Oliveira-Santos, C., Mews, H. A., Lopez-Gonzalez, G., Lloyd, J., Franczak, D. D., de Oliveira, E. A., Maracahipes, L., Miguel, A., Lenza, E., & Phillips, O. L. (2014). Disequilibrium and hyperdynamic tree turnover at the forest–cerrado transition zone in southern Amazonia. *Plant Ecology & Diversity*, *7*(1–2), 281–292. <https://doi.org/10.1080/17550874.2013.818072>
- Marimon, B. S., Oliveira-Santos, C., Marimon-Junior, B. H., Elias, F., de Oliveira, E. A., Morandi, P. S., S. Prestes, N. C. C. D., Mariano, L. H., Pereira, O. R., Feldpausch, T. R., & Phillips, O. L. (2020). Drought generates large, long-term changes in tree and liana regeneration in a monodominant Amazon forest. *Plant Ecology*, 1–15. <https://doi.org/10.1007/s11258-020-01047-8>
- Marimon-Junior, B. H., & Haridasan, M. (2005). Comparação da vegetação arbórea e características edáficas de um cerrado e um cerrado sensu stricto em áreas adjacentes sobre solo distrófico no leste de Mato Grosso, Brasil. *Acta Botanica Brasilica*, *19*, 913–926. <https://doi.org/10.1590/S0102-33062005000400026>
- Marimon-Junior, B. H., Hay, J. D. V., Oliveras, I., Jancoski, H., Umetsu, R. K., Feldpausch, T. R., Galbraith, D. R., Gloor, E. U., Phillips, O. L., & Marimon, B. S. (2019). Soil water-holding capacity and monodominance in Southern Amazon tropical forests. *Plant and Soil*, *450*, 65–79. <https://doi.org/10.1007/s11104-019-04257-w>
- Martínez-Vilalta, J., & Garcia-Forner, N. (2017). Water potential regulation, stomatal behavior and hydraulic transport under drought: Deconstructing the iso/anisohydric concept. *Plant, Cell & Environment*, *40*(6), 962–976.
- Martínez-Vilalta, J., Poyatos, R., Aguadé, D., Retana, J., & Mencuccini, M. (2014). A new look at water transport regulation in plants. *New Phytologist*, *204*(1), 105–115. <https://doi.org/10.1111/nph.12912>
- McDowell, N. G. (2011). Mechanisms linking drought, hydraulics, carbon metabolism, and vegetation mortality. *Plant Physiology*, *155*, 1051–1059. <https://doi.org/10.1104/pp.110.170704>
- Messier, J., McGill, B. J., & Lechowicz, M. J. (2010). How do traits vary across ecological scales? A case for trait-based ecology. *Ecology Letters*, *13*, 838–848. <https://doi.org/10.1111/j.1461-0248.2010.01476.x>
- Morandi, P. S., Marimon-Junior, B. H., De Oliveira, E. A., Reis, S. M., Valadão, M. B. X., Forsthofer, M., Passos, F. B., & Marimon, B. S. (2016). Vegetation succession in the Cerrado-Amazonian forest transition zone of Mato Grosso state, Brazil. *Edinburgh Journal of Botany*, *73*(1), 83–93. <https://doi.org/10.1017/S096042861500027X>
- Oliveira, R. S., Christoffersen, B. O., de V. Barros, F., Teodoro, G. S., Bittencourt, P., Brum-Jr, M. M., & Viani, R. A. G. (2014). Changing precipitation regimes and the water and carbon economies of trees. *Theoretical and Experimental Plant Physiology*, *26*(1), 65–82. <https://doi.org/10.1007/s40626-014-0007-1>
- Oliveira, R. S., Dawson, T. E., Burgess, S. S., & Nepstad, D. C. (2005). Hydraulic redistribution in three Amazonian trees. *Oecologia*, *145*(3), 354–363. <https://doi.org/10.1007/s00442-005-0108-2>
- Oliveira, R. S., Eller, C. B., De, F., Barros, V., Hirota, M., Brum, M., & Bittencourt, P. (2021). Linking plant hydraulics and the fast-slow continuum to understand resilience to drought in tropical ecosystems. *New Phytologist*, *230*, 904–923. <https://doi.org/10.1111/nph.17266>
- Oliveras Menor, I., & Jancoski, H. (2021). Leaf water potential Cerrado and Semideciduous forest. *Dryad*. <https://doi.org/10.5061/dryad.v41ns1rxp>
- Palhares, D., Franco, A. C., & Zaidan, L. B. P. (2010). Respostas fotossintéticas de plantas do cerrado nas estações seca e chuvosa. *Revista Brasileira De Biociências*, *8*(2), 213–220.
- Peixoto, K. S., Marimon-Junior, B. H., Cavalheiro, K. A., Silva, N., Neves, E. C., Freitag, R., Mews, H. A., Valadão, M. B. X., & Marimon, B. S. (2018). Assessing the effects of rainfall reduction on litterfall and the litter layer in phytophysiologicals of the Amazonia-Cerrado

- transition. *Brazilian Journal of Botany*, 41, 589–600. <https://doi.org/10.1007/s40415-018-0443-2>
- Prado, C. H. B. D. A., Wenhui, Z., Cardoza Rojas, M. H., & Souza, G. M. (2004). Seasonal leaf gas exchange and water potential in a woody cerrado species community. *Brazilian Journal of Plant Physiology*, 16(1), 7–16. <https://doi.org/10.1590/S1677-04202004000100002>
- R Core Team (2020). *R: A language and environment for statistical computing*. R Foundation for Statistical Computing.
- Ratter, J. A. (1971). Some notes on two types of cerrado occurring in northeastern Mato Grosso. In M. G. Ferri (Ed.), *III Simpósio sobre o Cerrado* (pp. 100–102). Edgard Blucher.
- Ratzmann, G., Zakrarova, L., & Tietjen, B. (2019). Optimal leaf water status regulation of plants in drylands. *Scientific Reports*, 9, 3768.
- Reis, S. M., Marimon, B. S., Marimon Junior, B. H., Mornadi, P. S., Oliveira, E. A., Elias, F., Neves, E. C., Oliveira, B., Nogueira, D. S., Umetsu, R. K., Feldpausch, T. R., & Oliver, L. P. (2018). Climate and fragmentation affect forest structure at the southern border of Amazonia. *Plant Ecology & Diversity*, 10, 1–11. <https://doi.org/10.1080/17550874.2018.1455230>
- Ribeiro, J. F., & Walter, B. M. T. (1998). Fitofisionomias do bioma Cerrado. In S. M. Sano & S. P. Almeida (Eds.), *Cerrado: ambiente e flora* (pp. 89–166). EMBRAPA/CPAC.
- Rifai, S. W., Girardin, C. A. J., Berenguer, E., del Aguila-Pasquel, J., Dahlsjö, C. A. L., Doughty, C. E., Jeffery, K. J., Moore, S., Oliveras, I., Riutta, T., Rowland, L. M., Murakami, A. A., Addo-Danso, S. D., Brando, P., Burton, C., Ondo, F. E., Duah-Gyamfi, A., Amézquita, F. F., Freitag, R., ... Malhi, Y. (2018). ENSO drives interannual variation of forest woody growth across the tropics. *Philosophical Transactions of the Royal Society B: Biological Sciences*, 373(1760), 20170410. <https://doi.org/10.1098/rstb.2017.0410>
- Scholander, P. F., Bradstreet, E. D., Hemmingsen, E., & Hammel, H. (1965). Sap pressure in vascular plants: Negative hydrostatic pressure can be measured in plants. *Science*, 148(3668), 339–346.
- Scholz, F. G., Bucci, S. J., Arias, N., Meinzer, F. C., & Goldstein, G. (2012). Osmotic and elastic adjustments in cold desert shrubs differing in rooting depth: Coping with drought and subzero temperatures. *Oecologia*, 170, 885–897. <https://doi.org/10.1007/s00442-012-2368-y>
- Scholz, F. G., Bucci, S. J., Goldstein, G., Meinzer, F. C., & Franco, A. C. (2002). Hydraulic Redistribution of soil water by Neotropical savanna trees. *Tree Physiology*, 22, 603–612. <https://doi.org/10.1093/treephys/22.9.603>
- Shepherd, G. J. (2010). *FITOPAC. Versão 2.1*. Departamento de Botânica, Universidade Estadual de Campinas-UNICAMP.
- Tardieu, F., & Simonneau, T. (1998). Variability among species of stomatal control under fluctuating soil water status and evaporative demand: Modelling isohydric and anisohydric behaviors. *Journal of Experimental Botany*, 49, 419–432.
- Taudiere, A., & Violle, C. (2015). cati: an R package using functional traits to detect and quantify multi-level community assembly processes. *Ecography*, 39, 699–708. <https://doi.org/10.1111/ecog.01433>
- Tyree, M. T. (2003). Plant hydraulics: the ascent of water. *Nature*, 423, 923. <https://doi.org/10.1038/423923a>
- Warton, D. I., Duursma, R. A., Falster, D. S., & Taskinen, S. (2012). smatr 3—an R package for estimation and inference about allometric lines. *Methods in Ecology and Evolution*, 3(2), 257–259.
- Wickham, H. (2011). The split-apply-combine strategy for data analysis. *Journal of Statistical Software*, 40, 1–29.

SUPPORTING INFORMATION

Additional supporting information may be found in the online version of the article at the publisher's website.

How to cite this article: Soares Jancoski, H., Schwantes Marimon, B., C. Scalón, M., de V. Barros, F., Marimon-Junior, B. H., Carvalho, E., S. Oliveira, R., & Oliveras Menor, I. (2022). Distinct leaf water potential regulation of tree species and vegetation types across the Cerrado–Amazonia transition. *Biotropica*, 54, 431–443. <https://doi.org/10.1111/btp.13064>